

Observation of breather excitons and soliton in a substituted polythiophene with a degenerate ground state

Takayoshi Kobayashi,^{1,2,3,4} Juan Du,^{1,2} Wei Feng,⁵ Katsumi Yoshino,⁶ Sergei Tretiak,⁷ Avadh Saxena,⁷ and Alan R. Bishop⁷

¹*Department of Applied Physics and Chemistry and Institute for Laser Science, University of Electro-Communications, 1-5-1 Chofugaoka, Chofu, Tokyo 182-8585, Japan*

²*JST, ICORP, Ultrashort Pulse Laser Project, 4-1-8 Honcho, Kawaguchi, Saitama 332-0012, Japan*

³*Department of Electrophysics, National Chiao Tung University, 1001 Ta Hsueh Road, Hsin-Chu 3005, Taiwan*

⁴*Institute of Laser Engineering, Osaka University, 2-6 Yamada-Oka, Suita, Osaka 565-0871, Japan*

⁵*School of Materials Science and Engineering, Tianjin University, Tianjin 300072, People's Republic of China*

⁶*Shimane Institute for Industrial Technology, 1 Hokuryo-cho, Matsue, Shimane 690-0816, Japan*

⁷*Theoretical Division and Center for Nonlinear Studies, Los Alamos National Laboratory, Los Alamos, New Mexico 87545, USA*

(Received 25 October 2009; revised manuscript received 22 December 2009; published 5 February 2010)

We investigated the ultrafast dynamics of a unique polythiophene derivative that has a degenerate ground state due to an alternating benzenoid-quinoid resonance. We probed 128 different wavelengths at the same time by using a sub-5-fs pulse laser and a detection system composed of a polychromator and a multichannel lock-in amplifier. The method allowed us to study the electronic relaxation and vibrational dynamics in completely same conditions at the same time. Because the polythiophene derivative has degenerate ground state, solitons are expected to be generated after photoexcitation. The dynamics of a breather composed of a dynamic bound state of solitons generated immediately after photoexcitation was time-resolved to reveal coupling between the vibrational modes and the solitons. The C—C and C=C stretching modes were found to be modulated by the breather, whose lifetime was determined to be 30–50 fs. The results of quantum-chemical excited-state molecular dynamics simulation are consistent with experimental results. Our modeling results allow to identify related vibrational normal modes strongly coupled to the electronic degrees of freedom. Moreover, analysis of calculated trajectories of excited state shows appearance of short-lived breather excitation decaying due to intramolecular vibrational energy equilibration on a time scale of hundreds of femtoseconds, which also agrees well with the experimental results.

DOI: [10.1103/PhysRevB.81.075205](https://doi.org/10.1103/PhysRevB.81.075205)

PACS number(s): 78.47.J-, 78.40.Me

I. INTRODUCTION

Unusual wave propagation, later termed a soliton, was first discovered in 1844.¹ Solitons have been identified in many fields of nonlinear physics^{2–7} including water waves, sound waves, matter waves, and electromagnetic waves.⁸ According to simulations performed using the Su-Schrieffer-Heeger (SSH) Hamiltonian,⁹ a photogenerated electron-hole ($e-h$) pair evolves into a soliton-antisoliton pair ($S\bar{S}$) within 100 fs after photoexcitation because of barrier-free relaxation in a one-dimensional system. Matter-wave solitons have given rise to many interesting phenomena in the simplest conducting polymer, *trans*-polyacetylene,¹⁰ including anomalous conductivity and huge optical nonlinearity.¹¹ The formation times of solitons in polyacetylene have been determined to be <150 fs.¹² Even though the existence of a soliton in *trans*-polyacetylene is well known and has been extensively studied, there has been no systematic study of conjugated polymer systems besides *trans*-polyacetylene. This is probably because of the scarcity of polymers with a degenerate ground state.

It has also been theoretically predicted^{9,13–16} that the soliton pair is spatially localized to form a dynamic bound state called a breather. The excess energy of the photogenerated ($e-h$) pair over that of the soliton pair induces collective carbon-carbon (C—C) oscillations, namely, the breather mode, due to electron-phonon coupling. Breathers predicted in Ref. 17 have been observed in *trans*-polyacetylene,¹⁸

which was found to have a period of 44 fs and an extremely short lifetime of ~ 50 fs. However, there is not yet currently consensus among researchers as to whether breather is the primary photogenerated excitations and how they affect the ultrafast vibronic dynamics.^{18–22}

In this paper, we report the study of the dynamics of solitons and breather in a quinoid-benzenoid polythiophene with a degenerate ground state which chemical structure is shown in Fig. 1(a). It is well-known that polythiophene is one of the most promising materials for various device applications, so that a detailed understanding of the dynamics of electronic state and vibrational dynamics photoexcitations in them and their derivatives is highly desirable for practical reasons. The polymer system studied in the present paper appears ostensibly not to have a degenerate ground state, however, it has degeneracy due to the tautomerization of the inner structure of the polymer, as described below. And its repeat unit is much larger than that of *trans*-polyacetylene. The repeat unit in the latter is composed of one single bond and one double bond, while the one in the former is more bulky since it has two thiophene rings with both *cis* and *trans* configurations. Since there has been no other spectroscopic study of solitons except for *trans*-polyacetylene before, it is of great interest to study its dynamics and compare any differences between it and *trans*-polyacetylene in terms of the repeat unit structure. To the best of our knowledge, this is the first observation of the existence of a breathe and solitons and their dynamics in a system other than *trans*-polyacetylene. To rationalize the

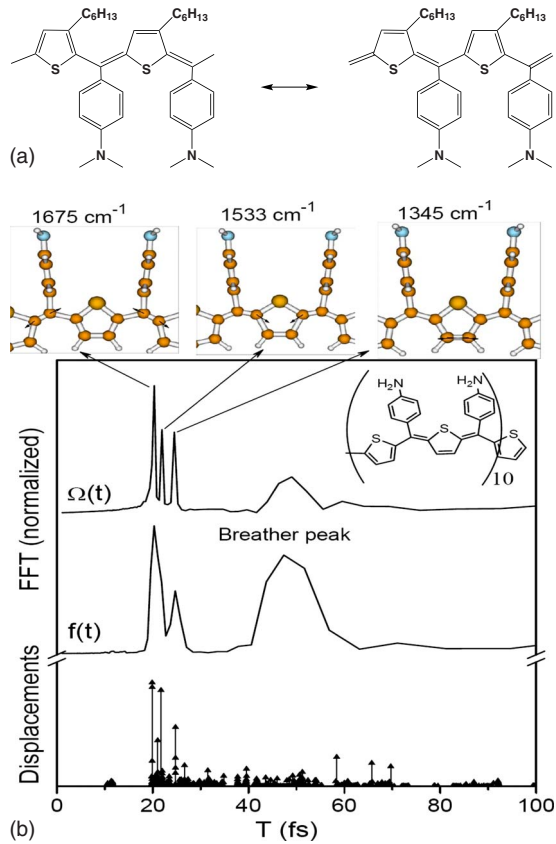


FIG. 1. (Color online) Two quantum-mechanical resonant structures of (a) PHTDMABQ and (b) the excited-state molecular dynamics simulations results. (b) shows the normalized Fourier spectra of the lowest dipolar allowed excited-state transition energy $\Omega(t)$ and its respective oscillator strength $f(t)$ trajectories (top two plots), and the amplitudes of dimensionless displacements Δ (stick spectrum, bottom panel) along normal modes calculated in the oligomer with 10 repeat units, as shown in the inset. The three molecular structures at the top schematically show vibrational normal modes with frequencies strongly coupled to the electronic system, which lead to the formation of the breather excitation. These correspond to the C=C vibration and C—C stretches as schematically shown in the middle panel.

experimental data, we performed a quantum-chemical excited-state molecular dynamics simulation, and its results are consistent with experimental data, enabling breather excitations to be analyzed and related coupled vibrational normal modes to be identified.

II. EXPERIMENTAL DESCRIPTION

In the present experiment, we utilized a nearly Fourier-transform limited visible-near-IR pulse generated from a noncollinear optical parametric amplifier (NOPA) seeded by a white-light continuum, as shown in Fig. 2. The pump source of this NOPA system was a regenerative amplifier (Spectra Physics, Spitfire) with the following operating parameters: central wavelength, 800 nm; pulse duration, 50 fs; repetition rate, 5 kHz; average output power, 650 mW. We used a 1-mm-thick sapphire plate to generate the continuum

spectrum, and great care was taken to introduce only the formation of a single filament. The NOPA output pulse was compressed with a pair of chirp mirrors and then with a prism pair, resulting in a nearly Fourier transform (FT) limited pulse duration of 6.3 fs. Both the pump and probe pulses covered the spectral range extending from 515 to 716 nm,²³ and the energies of them are about 50 and 6 nJ, respectively. The pump-probe signal at 128 different wavelengths was detected by a combined system of a polychromator and a multichannel lock-in amplifier. Thanks to the extreme stability of the light source and noise reduction by the lock-in-detector, the time resolution is better than 1 fs, which was recognized by the difference between the time-resolved spectra at neighboring delay step obtained using the time step of 0.2 fs.

The sample studied in this study was a thin film of quinoid-benzenoid polythiophene, poly[3-hexylthiophene-2,5-diyl]-[*p*-dimethylaminobenzylidenequinoidmethene] (PHTDMABQ), which was dissolved in methanol and cast on a quartz substrate for stationary and time-resolved spectra measurements. All experiments were performed at room temperature (293 ± 1 K).

III. MOLECULE STRUCTURE

The structure of PHTDMABQ is depicted in Fig. 1(a), whose monomer is a derivative of thiophene. It appears ostensibly not to have a degenerate ground state. There is no degenerate ground state in polythiophene because quinoid thiophene has a higher energy than benzenoid thiophene. Therefore, it has a benzenoid structured ground state. After photoexcitation, this benzenoid structure is converted into a quinoid structure, but this excitation with the latter structure cannot propagate freely along the polymer chain, unlike solitons in *trans*-polyacetylene. Thus, the absence of solitons in polythiophenes is due to the energy difference between benzenoid thiophene and quinoid thiophene. Bipolarons are generated by photoexcitation. The two polarons in the bipolarons cannot be separated from each other because they are nondegenerate. However, in the case of PHTDMABQ, there are two tautomers, benzenoid and quinoid. Both the benzenoid thiophene and quinoid thiophene are next to each other, to form a repeat unit and they can exchange their tautomeric structures without energy requirement. Therefore, the ground state can be either $\{ \text{quinoid-benzenoid} \}_n$ or $\{ \text{benzenoid-quinoid} \}_n$ as shown in Fig. 1(a). Because of the tautomerization of the internal structure of PHTDMABQ, it can have a degenerate ground state and thus solitons can be generated in it.

IV. QUANTUM-CHEMICAL METHODOLOGY

To analyze the experimental data, we used the Austin Model 1 (AM1) Hamiltonian and an excited-state molecular dynamics (ESMD) computational package, which is described in detail in Refs. 24 and 25, to follow photoexcitation adiabatic dynamics on a picosecond time scale for all calculations presented in this study. The ESMD approach calculates the excited-state potential energy as $E_e(\mathbf{q}) = E_g(\mathbf{q}) + \Omega(\mathbf{q})$ in the space of nuclear coordinates \mathbf{q} that span the

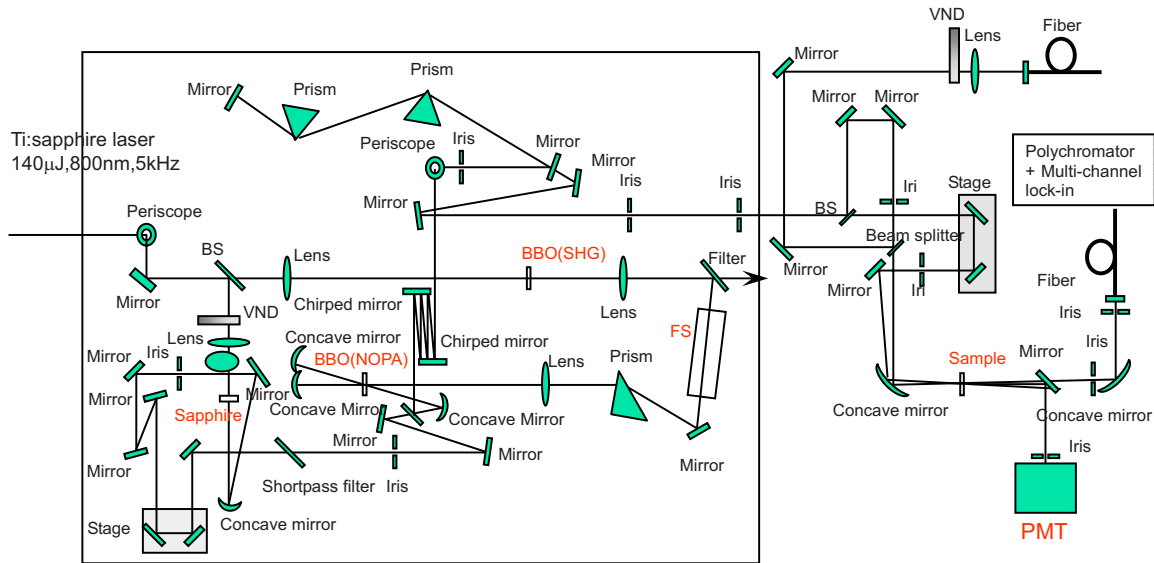


FIG. 2. (Color online) Block diagram of the apparatus of vibration real-time spectroscopy based on a pump-probe scheme. VND: variable neutral-density filter; FS: fused silica; BS: beam splitter.

entire ($3N-6$) dimensional space, where N is the total number of atoms in the molecule. Here, $\Omega(\mathbf{q})$ is the electronic transition frequency to the lowest $1B_u$ (band-gap) state of the photoexcited molecule. The program efficiently calculates analytical derivatives of $E_e(\mathbf{q})$ with respect to each nuclear coordinate q_i to evaluate forces and to subsequently step along the excited-state hypersurface using these gradients. All computations start from vertical excitation at the optimal ground-state molecular geometry. The total molecular energy $E_e(\mathbf{q})$ is conserved if no dissipative processes are included. Subsequent analysis of the photoexcited trajectories of the excitation energy $\Omega(\mathbf{q}, t)$ and oscillator strength $f(\mathbf{q}, t)$ in Fourier space allows us to identify periods of participating vibrational motions. Alternatively, the minimum of the excited-state potential energy surface can be calculated by including an artificial dissipative force in the equations of motion corresponding to the relaxed excited-state geometry. To understand the formation of photoexcited breathers, we calculated the dynamics of the band-gap excited state in the 10-unit thiophene oligomer shown in the inset of Fig. 1(b), where the alkyl side chain have been replaced by hydrogens, effectively reducing the molecular size for calculations. This molecule is sufficiently long (10 nm) compared to the characteristic exciton size of about 2 nm for the infinite chain limit to be valid.

V. RESULTS AND DISCUSSION

A. Vibrational real-time spectra and analysis

As described in the Experimental section, the stability of our NOPA laser and 128 channel-lock-in amplifiers helps us in very detailed analysis of dynamics of both electronic relaxation and real-time molecular vibration. In order to obtain a complete view of excited-state evolution triggered by the ultrashort pulse, it is of vital importance to measure the dynamics at different probe wavelength to obtain most reliable

information by the experiment to be performed. High sensitivity can be achieved by using a lock-in amplifier based on a phase-sensitive detection scheme, but in traditional experiment it is performed by single wavelength measurement. Spectroscopic measurement can be performed by using a linear array detector or two-dimensional detector such as CCD camera. However, in this method is not based on the phase-sensitive detection scheme, the data accumulate associated background noise and the data acquisition time is limited by the overflow of noise accumulated. The method of the present paper is not suffered from this problem.

The method presented in this paper is based on the modulation of transmitted light intensity induced by molecular vibration. This modulation can be classified into three mechanisms. One is the transition intensity change in probing wavelength due to “vibronic coupling.” In this case the amount of the transmission intensity change is proportional to the coupling strength and vibrational amplitude. The second one is the amplification and deamplification of the probe light induced by the stimulated Raman process. The third one is due to the modulation of the refractive index associated with molecular vibration resulting in the spectral shift proportional to the change in the refractive index and hence to the change in the phase velocity.

The transition probability change due to the “vibronic coupling” mechanism above mentioned is classified again into two subgroups.²⁶ The first subgroup is Condon-type in which the change in the transmitted light intensity to be observed is proportional to the first derivative of the absorption (or emission) spectrum depending on the relative configuration of the potential curves of the relevant initial and final states of absorption (or emission). The first subgroup is again into potential-minimum-shift type and potential-curvature-change type. The probe wavelength dependence of amplitudes of the Fourier transform of the former and the latter are obtained by the first and second derivative of the relevant electronic transition spectra, respectively. The second sub

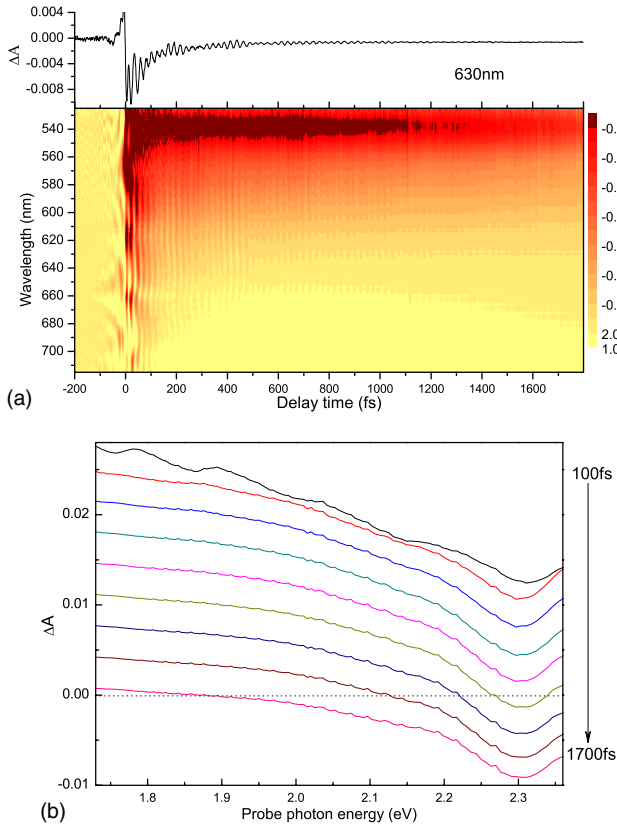


FIG. 3. (Color online) (a) Two-dimensional real-time absorbance change. One example of the time-dependent absorbance change at 630 nm was plotted as the top figure. (b) The time-resolved pump-probe spectra probed at 10 center delay time points from 100 to 1700 fs with an integration time width of 200 fs.

group is non-Condon type, in which the vibration modulate the transition dipole moment and hence the transmitted light intensity change is proportional to the zero-th derivative of the absorption (or emission) spectrum.

The method can provide the information of the change in intensity of absorption (or emission) as a function of probe frequency $\Delta A(\omega)$ from which the electronic relaxation is studied. The signal shows the decay dynamics and spectral change associated with the change in the electronic state. On top of that signal the modulation $\delta\Delta A(\omega)$ of the $\Delta A(\omega)$ due to molecular vibration can be used to study the vibrational dynamics of the system completely in the same condition as that electronic dynamics study. This situation is difficult to be realized in experiment made by using conventional UV (VIS) pump-UV (VIS) probe experiment and time-resolved vibrational experiment. In this paper the decay dynamics of the electronic state and vibrational dynamics highly correlated through excitonic coupling (vibronic coupling) were observed under the same condition at the same time.

B. Electronic relaxation and molecular vibration dynamics

The difference absorbance (ΔA) signals in Fig. 3(a) exhibit oscillation due to molecular vibrations. As shown in the ΔA traces, the lifetimes of the electronic states consist of three components: 62 ± 2 fs, 750 ± 20 fs, and >3 ps.²⁷ The

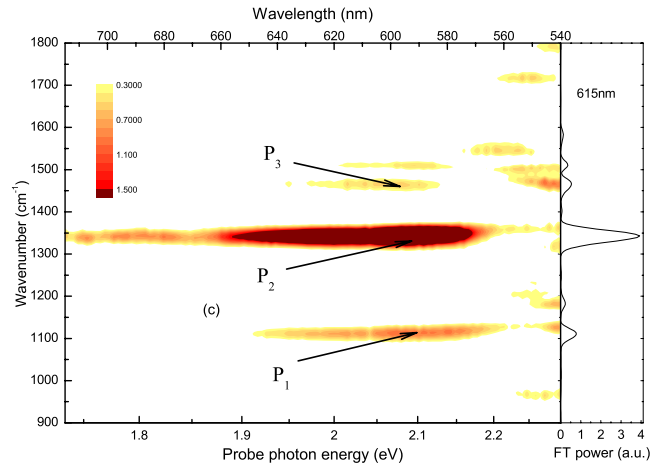


FIG. 4. (Color online) Fourier-transform power spectra. The Fourier-transform power spectrum at 615 nm is plotted as an example.

Fourier power spectra in Fig. 4 have peaks at 1111 ± 7 , 1343 ± 7 , and 1465 ± 7 cm^{-1} (P_1 , P_2 , and P_3 , respectively).

Theoretical calculations allow assigning these peaks to C—C stretching modes with different bond orders. Figure 1(b) shows the calculated dimensionless displacements Δ along the vibrational coordinates of the optimal geometries between the ground and excited states. This immediately enables us to identify the P_1 – P_3 vibrational normal modes that are strongly coupled to the electronic excitation. These correspond to intra- and interthiophene ring C—C and C=C stretching motions [see Fig. 1(b), top structures]. The highest, medium, and lowest frequencies are considered to correspond to C=C double bonds, a mixture of double and single bonds, and single bonds, respectively. The calculated vibrational frequencies (1345 , 1533 , and 1675 cm^{-1}) are overestimated by about 200 cm^{-1} compared to the experimental values, which is typical for semiempirical calculations.

C. Dynamics of breather and soliton

The requirement for the existence of solitons is a degenerate ground-state structure, and as shown in Fig. 1(a), our quinoid-benzenoid polythiophene sample has a degenerate ground state because the two quantum-mechanical resonance structures have equivalent energies. In Fig. 3(b), the transient absorption spectra exhibit negative absorbance changes in the photon energy range 1.91 to 2.38 eV, while for photon energies smaller than 1.91 eV, the absorbance change is positive. This increase in the absorbance is attributed to the tail of the solitons not fully relaxing to the band-gap center, as is the case in *trans*-polyacetylene.¹⁸ Therefore, the induced absorption observed in poly-(substituted thiophene) is attributed to solitons. The positive value indicates the increased contribution of induced absorption due to a soliton with a peak near the mid gap, which is estimated to be around 1.4 eV.

Spectrogram is an analysis method of the time-dependent spectrum where the instantaneous frequency changes with time. It is suited to study the dynamic process where the

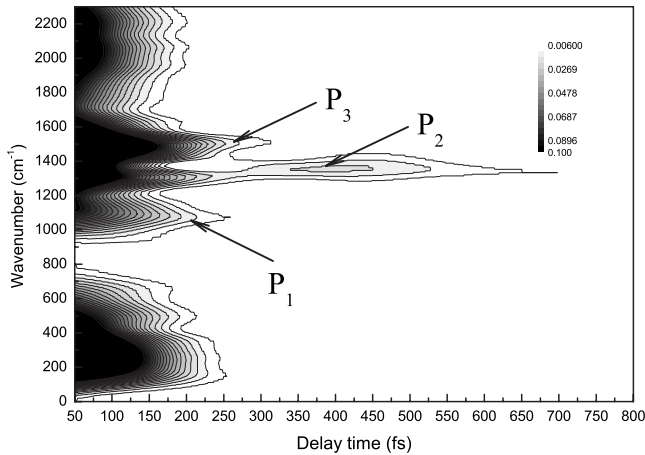


FIG. 5. Contour maps of the two-dimensional Fourier power of the vibrational components obtained by spectrogram calculation for real-time data covering 680–690 nm.

molecular geometrical relaxation or chemical reaction is accompanied with change in its vibrational frequency due to molecular structural change during the processes. Figure 5 shows the contour map obtained by the spectrogram analysis,²⁸ it has three prominent peaks corresponding to peaks P_1 , P_2 , and P_3 . In addition to these three modes, five more peaks appear as side bands of P_1 – P_3 at 270, 500, 640, 1960, and 2200 cm^{-1} . These five modes are breather modes which are not visible in the two-dimensional Fourier power spectrum (Fig. 4) or in the stationary resonance Raman spectrum because they have extremely broad widths due to their short lifetimes. In other words, the breather cannot appear in Raman spectra because it is a short-lived transient vibration mode, and hence it is not a normal mode or eigenmode. We also note that there are no detectable normal modes with substantial intensity in this spectral region coupled to the electronic excitation as evidenced by lack of significant displacements calculated in Fig. 1(b). The amplitudes of the high-frequency modes in the 2000–2200 cm^{-1} range decrease rapidly due to their short vibrational periods, which cannot be properly resolved by the finite pulse widths of both pump and probe pulses. However, the frequency is not affected and the breather excitation is clearly visible for the three sidebands with the lower frequencies.

The average frequency difference between the three main bands (1111, 1343, and 1465 cm^{-1} and their corresponding side bands (270 and 1960 cm^{-1} for 1111 cm^{-1} , 500, and 2200 cm^{-1} for 1343 cm^{-1} , and 640 cm^{-1} for 1465 cm^{-1}) is calculated to be 843 ± 12 cm^{-1} , which is close to the experimentally observed value of about 760 cm^{-1} reported for polyacetylene,¹⁸ and theoretically expected values of 660–1000 cm^{-1} .^{14–17} This frequency separation between the main bands and the satellite bands indicates that the breather modulates the C—C stretching modes with a period of ~ 40 fs generating the sidebands. The reason why the mode with frequency of 1465 cm^{-1} has only one lower sideband is because of the reduced intensity of upper sideband expected to be located around 2308 cm^{-1} corresponding to 14.4 fs close to the convoluted duration (8.9 fs) of the pulse duration time of both pump and probe pulses. Because of the limited

time resolution, the upper band signal could not be observed.

The lifetimes of the side bands were determined to be about 50, 32, and 40 fs for sidebands of P_1 , P_2 , and P_3 , respectively. They are corresponding to the life time of the breather mode as observed decay time of 50 fs in polyacetylene.¹⁸ The theoretically predicted decay time is shorter than 100 fs is again consistent with our observation. The result means the time for the breather mode to disappear followed by the separation into isolated solitons, and even shorter than that in polyacetylene. These short lifetimes are also corresponding to the shortest lifetime component of ~ 62 fs in the ΔA trace.²⁷ The ultrafast relaxation of ~ 50 fs of this nonlinear excitation ensures an ultrafast nonlinear response that can be used in all-optical switches.

Consequently, these sideband peaks appear due to nonlinear electron-vibrational excited-state dynamics. To analyze these processes from theoretical calculations, we compute the power spectra of 750 fs photoexcited trajectories of the excitation energy $\Omega(\mathbf{q}, t)$ and oscillator strength $f(\mathbf{q}, t)$ shown in Fig. 1(b).^{24,29} Both plots show an additional broad peak centered around 50 fs, corresponding to a vibration in the range 550 to 800 cm^{-1} , which does not correspond to any of the vibrational normal modes that exhibit substantial coupling to the electronic degrees of freedom [compare the displacements peaks with the fast Fourier transform (FFT) trajectories in Fig. 1(b)]. Based on our previous computational studies, we assign this peak to a nonlinear breather excitation that occurs due to coupling of C—C vibrational motions. This vibrational excitation decays gradually over long time scales due to dissipation of vibrational energy to internal vibrational degrees of freedom that are weakly coupled to the electronic system; this is similar to previous findings by us.^{24,29} Power spectra of longer excited-state trajectories (not shown) demonstrate diminishing breather peak. Our calculations estimate the breather lifetime to be about 0.2 ps without accounting for intermolecular dissipation channels (baths). Such fast decay is considered to be reasonably in agreement with our experiment data of ~ 50 fs, in case we take into accounts of both intermolecular interactions and phonon energy leakage through the boundaries of conjugated segments (defects). These processes may reduce breather lifetime from 0.2 ps to ~ 50 fs.²⁹ As expected, the breather peak is more pronounced in the power spectrum of the oscillator strength (see Fig. 5), since it is directly related to the modulation of the respective transition dipole moment.²⁹

In the previous studied for breather in polyacetylene,¹⁸ we only measured the real-time traces at only four different probe wavelengths (620, 720, 740, and 750 nm). However, it was very difficult to study the probe wavelength dependence of the modes due to modulation because of the small number of probe wavelengths (i.e., probe photon energies). In the present study, thanks to the multichannel detection system developed, we could observe the molecular vibration induced modulation $\delta\Delta A$ of the absorbance change ΔA at 128 different wavelengths simultaneously. In this way, the probe wavelength dependence can be used in detailed discussions on the photon energy dependence of modulation amplitudes of various modes. As shown in Fig. 6, the breather strongly contributes to the variations in the oscillator strength. Except

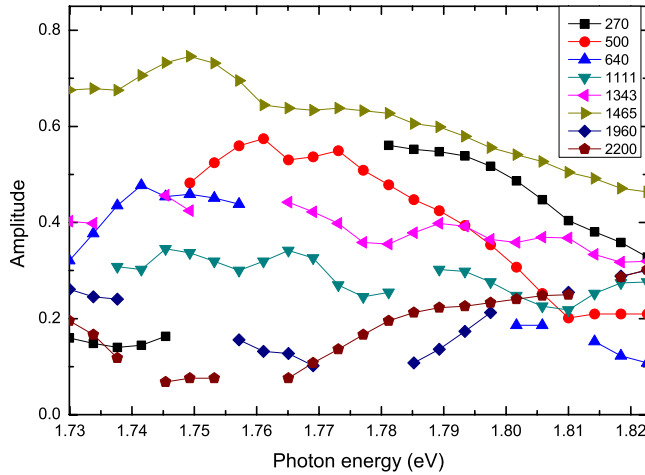


FIG. 6. (Color online) The probe photon energy dependence of the vibrational amplitude probed at a 110 fs gate delay time with a gate width of 120 fs (half-width at half maximum) in the spectrogram.

for the modes at 1960 and 2200 cm^{-1} , the signal sizes of all the modes exhibit an almost monotonic increase when the photon energy is reduced from 1.82 to 1.73 eV. This is consistent with the theoretical discussion in Ref. 24. Similar feature is found for the positive absorbance change, as shown in Fig. 3(b). The magnitude of the positive absorbance change increases when the probe photon energy decreases. This provides the evidence of the larger contribution of the breather to the modulation ($\delta\Delta A$) of the difference absorbance change (ΔA) due to soliton in the lower energy range. We can interpret this feature in terms of the modulation of the transient spectrum of soliton by the vibrational modes as follows.

Molecular vibration associated with the breather and soliton is expected to modulate the transition energy and transition probability, and the amplitudes are expected to be proportional to the zeroth, first, and second derivatives of the absorption and/or stimulated emission spectrum depending on the mechanism of induction of the wavepacket motions.³⁰ Since the absorption spectrum of soliton is expected to be close to the mid gap, which is located at 1.4 eV in the case of polyacetylene, the spectral range of the present observation is higher energy tail of the soliton absorption as seen from the time-resolved spectrum as shown in Fig. 3(b). Therefore, all of the zeroth, first, and second derivatives of the absorption spectrum are expected to increase monotonically with decreasing probe photon energy.

Here, we go back to the discussion of the above mentioned exceptional behavior of the probe wavelength dependence of the amplitudes of the two modes at 1960 and 2200 cm^{-1} . It can be explained in the following way. The molecular vibration modulates the transition probability and transition energy because of the electronic distribution change nearly instantaneously following the motion of nuclei

during the molecular vibration. The frequencies of the modes at 1960 and 2200 cm^{-1} are nearly equal to the overtones of 1111 cm^{-1} , which may affect the dynamics of the breather. The electronic transition is modulated at periodically with period of ~ 30 , 17, and 15 fs corresponding to the frequencies of 1111, 1960, and 2200 cm^{-1} , respectively. Then, at integer multiple of about 32 fs, all of them contribute. In case the vibrations of the modes are in-phase or out-of-phase then the amplitudes of them may be affected by either constructive or destructive interference.

We now discuss the effect of the differences in the sizes and structures of the repeat units. The repeat unit in the *trans*-polyacetylene is composed of one single bond and one double bond, while in PHTDMABQ, it is composed of two thiophene rings, which show antiphase tautomerism (see Fig. 1), which produces the degenerate ground state in the polymer. Since PHTDMABQ has a *cis* configuration in the thiophene ring, it is interesting to compare it with *cis*-polyacetylene. The lifetime of breather is expected to be longer than that in *trans*-polyacetylene. However, the decay time of the breather seems to be even shorter than that in *trans*-polyacetylene. That is because the lifetime is not determined by the separation of soliton pairs from the originally generated site in the polymer chain, but by the energy dissipation to internal vibrational freedom. Since quinoid-benzenoid polythiophene has many more internal vibrational modes than *trans*-polyacetylene, its breather lifetime is even shorter than that of *trans*-polyacetylene.

VI. CONCLUSIONS

In summary, using a polythiophene derivative with a degenerate ground state, we investigated the ultrafast dynamics that take place immediately after excitation. The simulation results of quantum-chemical excited-state molecular dynamics agree reasonably well with the experimental data by showing formation of short-lived breather excitation. The breather lifetime was experimentally determined from the electronic spectral dynamics to be ~ 62 fs, which agrees with the time constants determined by the time-dependent signal intensity that appears as side peaks associated with the breather. Even though extensive theoretical studies have been conducted, to the best of our knowledge, this is the first time that modulation of the C—C single and double stretching modes by the breather have been experimentally observed other than in *trans*-polyacetylene.

ACKNOWLEDGMENTS

This work was partly supported by a grant from the Ministry of Education (MOE) in Taiwan under the ATU Program at National Chiao Tung University. A part of this work was performed under the joint research project of the Institute of Laser Engineering, Osaka University under Contract No. B1-27.

- ¹J. S. Russell, in *Report of the Fourteenth Meeting of the British Association for the Advancement of Science* (Murray, London, 1844), pp. 311-390.
- ²N. Manton and P. Sutcliffe, *Topological Solitons* (Cambridge University Press, Cambridge, England, 2004).
- ³L. Khaykovich, F. Schreck, G. Ferrari, T. Bourdel, J. Cubizolles, L. D. Carr, Y. Castin, and C. Salomon, *Science* **296**, 1290 (2002).
- ⁴K. E. Strecker, G. B. Partridge, A. G. Truscott, and R. G. Hulet, *Nature (London)* **417**, 150 (2002).
- ⁵M. Nakazawa, E. Yamada, and H. Kubota, *Phys. Rev. Lett.* **66**, 2625 (1991).
- ⁶W. P. Su, J. R. Schrieffer, and A. J. Heeger, *Phys. Rev. Lett.* **42**, 1698 (1979).
- ⁷A. M. Kosevich, B. A. Ivanov, and A. S. Kovalev, *Phys. Rep.* **194**, 117 (1990).
- ⁸G. I. Stegeman and M. Segev, *Science* **286**, 1518 (1999).
- ⁹W. P. Su and J. R. Schrieffer, *Proc. Natl. Acad. Sci. U.S.A.* **77**, 5626 (1980).
- ¹⁰H. Shirakawa, *Rev. Mod. Phys.* **73**, 713 (2001).
- ¹¹H. Naarmann and N. Theophilou, *Synth. Met.* **22**, 1 (1987).
- ¹²C. V. Shank, R. Yen, R. L. Fork, J. Orenstein, and G. L. Baker, *Phys. Rev. Lett.* **49**, 1660 (1982).
- ¹³D. K. Campbell, *Nature (London)* **432**, 455 (2004).
- ¹⁴M. Sasai and H. Fukutome, *Prog. Theor. Phys.* **79**, 61 (1988).
- ¹⁵S. R. Phillipot, A. R. Bishop, and B. Horovitz, *Phys. Rev. B* **40**, 1839 (1989).
- ¹⁶S. Block and H. W. Streitwolf, *J. Phys.: Condens. Matter* **8**, 889 (1996).
- ¹⁷A. R. Bishop, D. K. Campbell, P. S. Lomdahl, B. Horovitz, and S. R. Phillipot, *Phys. Rev. Lett.* **52**, 671 (1984).
- ¹⁸S. Adachi, V. M. Kobryanskii, and T. Kobayashi, *Phys. Rev. Lett.* **89**, 027401 (2002).
- ¹⁹G. S. Kanner, Z. V. Vardeny, G. Lanzani, and L. X. Zheng, *Synth. Met.* **116**, 71 (2001).
- ²⁰K. M. Gaab and C. J. Bardeen, *J. Phys. Chem. B* **108**, 4619 (2004).
- ²¹G. Lanzani, G. Cerullo, C. Brabec, and N. S. Sariciftci, *Phys. Rev. Lett.* **90**, 047402 (2003).
- ²²R. Lécuyer, J. Berréhar, C. Lapersonne-Meyer, and M. Schott, *Phys. Rev. Lett.* **80**, 4068 (1998).
- ²³A. Baltuška, T. Fuji, and T. Kobayashi, *Opt. Lett.* **27**, 306 (2002).
- ²⁴S. Tretiak, A. Saxena, R. L. Martin, and A. R. Bishop, *Proc. Natl. Acad. Sci. U.S.A.* **100**, 2185 (2003).
- ²⁵S. Tretiak, A. Saxena, R. L. Martin, and A. R. Bishop, *Phys. Rev. Lett.* **89**, 097402 (2002).
- ²⁶T. Kobayashi and Z. Wang, *IEEE J. Quantum Electron.* **44**, 1232 (2008).
- ²⁷J. Du, Z. Wang, W. Feng, K. Yoshino, and T. Kobayashi, *Phys. Rev. B* **77**, 195205 (2008).
- ²⁸M. J. J. Vrakking, D. M. Villeneuve, and A. Stolow, *Phys. Rev. A* **54**, R37 (1996).
- ²⁹S. Tretiak, A. Piryatinski, A. Saxena, R. L. Martin, and A. R. Bishop, *Phys. Rev. B* **70**, 233203 (2004).
- ³⁰T. Kobayashi, Z. Wang, and I. Iwakura, *New J. Phys.* **10**, 065009 (2008).